AD

TECHNICAL REPORT ARBRL-TR-02386

SENSITIVITY ANALYSIS OF MICHELSON TYPE MICROWAVE INTERFEROMETRY FOR THE MEASUREMENT OF PROJECTILE IN-BORE MOTION

Rurik K. Loder

January 1982

US ARMY ARMAMENT RESEARCH AND DEVELOPMENT COMMAND
BALLISTIC RESEARCH LABORATORY
ABERDEEN PROVING GROUND, MARYLAND

Destroy this report when it is no longer needed.
Do not return it to the originator.

Secondary distribution of this report by originating
or sponsoring activity is prohibited.

Additional copies of this report may be obtained
from the National Technical Information Service,
U.S. Department of Commerce, Springfield, Virginia
22161.

The findings in this report are not to be construed as
an official Department of the Army position, unless
so designated by other authorized documents.

*The use of trade names or manufacturers' names in this report
does not constitute indorsement of any commercial product.*

REPORT DOCUMENTATION PAGE		READ INSTRUCTIONS BEFORE COMPLETING FORM
1. REPORT NUMBER Technical Report ARBRL-TR-02386	2. GOVT ACCESSION NO.	3. RECIPIENT'S CATALOG NUMBER
4. TITLE (and Subtitle) SENSITIVITY ANALYSIS OF MICHELSON TYPE MICROWAVE INTERFEROMETRY FOR THE MEASUREMENT OF PROJECTILE IN-BORE MOTION		S. TYPE OF REPORT & PERIOD COVERED Technical Report
		6. PERFORMING ORG. REPORT NUMBER
7. AUTHOR(s) Rurik K. Loder		8. CONTRACT OR GRANT NUMBER(s)
9. PERFORMING ORGANIZATION NAME AND ADDRESS U.S. Army Ballistic Research Laboratory ATTN: DRDAR-BLI Aberdeen Proving Ground, MD 21005		10. PROGRAM ELEMENT, PROJECT, TASK AREA & WORK UNIT NUMBERS 1L162618AH80
11. CONTROLLING OFFICE NAME AND ADDRESS U.S. Army Armament Research & Development Command U.S. Army Ballistic Research Laboratory ATTN: DRDAR-BL Aberdeen Proving Ground, MD 21005		12. REPORT DATE January 1982
		13. NUMBER OF PAGES 33
14. MONITORING AGENCY NAME & ADDRESS(If different from Controlling Office)		15. SECURITY CLASS. (of this report) UNCLASSIFIED
		15e. DECLASSIFICATION/DOWNGRADING SCHEDULE

16. DISTRIBUTION STATEMENT (of this Report)

Approved for public release; distribution unlimited

17. DISTRIBUTION STATEMENT (of the abstract entered in Block 20, if different from Report)

18. SUPPLEMENTARY NOTES

19. KEY WORDS (Continue on reverse side if necessary and identify by block number)

Projectile Gun Dynamics
Projectile In-Bore Motion
Microwave Interferometry

20. ABSTRACT (Continue on reverse side if necessary and identify by block number)   jmk

Analysis of projectile-cannon interface problems quite often requires accurate determination of the projectile in-bore and launch motion. Microwave interferometry and Doppler radar are the two most commonly used instrumentation and measurement techniques for obtaining projectile travel and velocity. To determine whether microwave interferometry can be used for an accurate measurement of projectile in-bore travel, a sensitivity analysis is presented. It shows that the current, commonly used measurement procedures lead to errors

(continued)

20. (continued)

in projectile in-bore travel unacceptable for the analysis of projectile-cannon interface problems. However, the analysis reveals also that the maximum uncertainty in projectile travel can be reduced to less than one millimeter, if the microwave interferometry technique is employed diligently, with close attention given to the determination of the parameters in the guide wavelength equation.

TABLE OF CONTENTS

LIST OF ILLUSTRATIONS

5

LIST OF TABLES

I. INTRODUCTION

Microwave interferometry is extensively used for the measurement of travel and velocity of projectiles during their in-bore propulsion. Though this measurement technique has been with us for a long time, we have not reached the state where it can be exploited for the detailed analysis of projectile motion conveniently and in real time. In contrast to projectile free flight, where microwave measurement techniques are well established and Doppler radar signals are readily analyzable with stationary time series methods, the application of microwave techniques to monitor projectile in-bore motion is more difficult. This is caused by instrumentation to operate in the gun blast environment and by the requirement for the more complicated signals which present highly non-stationary time series and contain a conglomerate of physical information. Various instrumentation and data analysis methods have been and are being developed to overcome the difficulties. Basically, three types of microwave instrumentation are used for the recording of projectile in-bore motion: the Michelson type microwave interferometer with fixed frequency, the Doppler radar, and the microwave interferometer with variable frequency. The last one is a recent development[1].

Analysis of projectile-gun interface problems quite often requires accurate knowledge of the projectile in-bore and launch motion. The reduction of projectile-gun interface parameters such as pressure, bore traction, projectile alignment, etc. from recorded local tube strains, is one example. The analysis requires superposition of the elastic theory of thick walled cylinders on the strain data using general least squares model fitting procedures. One way to reduce the dimensions of the parameter vector and the constraint functions in the least squares model is the predetermination of the projectile motion by other means. The permissible error in projectile travel is less than one millimeter in the 105 mm M68 tank gun, for instance. To determine whether microwave measurement techniques can be used for such an accurate measurement of projectile travel, a relatively crude sensitivity analysis was conducted.

II. EXPERIMENTAL ARRANGEMENT

The experimental setup, as customarily deployed at the Interior Ballistics Division, represents a Michelson type microwave interferometer (Figure 2.1). A coherent microwave beam polarized in the vertical plane is radiated from the emitting antenna into the circular cylindrical waveguide with the free space wavelength λ_o. The waveguide propagates the microwave beam with the guide wavelength λ_g. The beam strikes

---

[1] H. Grumann, "A Microwave Interferometer With Variable Frequency For Continuous Determination of Projectile Motion", Proceedings of Workshop on Projectile-Gun Dynamics under the Auspices of the DEA-G-1060, Ballistics Research and Development, 24-26 April 1979, USA ARRADCOM, Ballistic Research Laboratory, Aberdeen Proving Ground, Maryland 21005 (to be published).
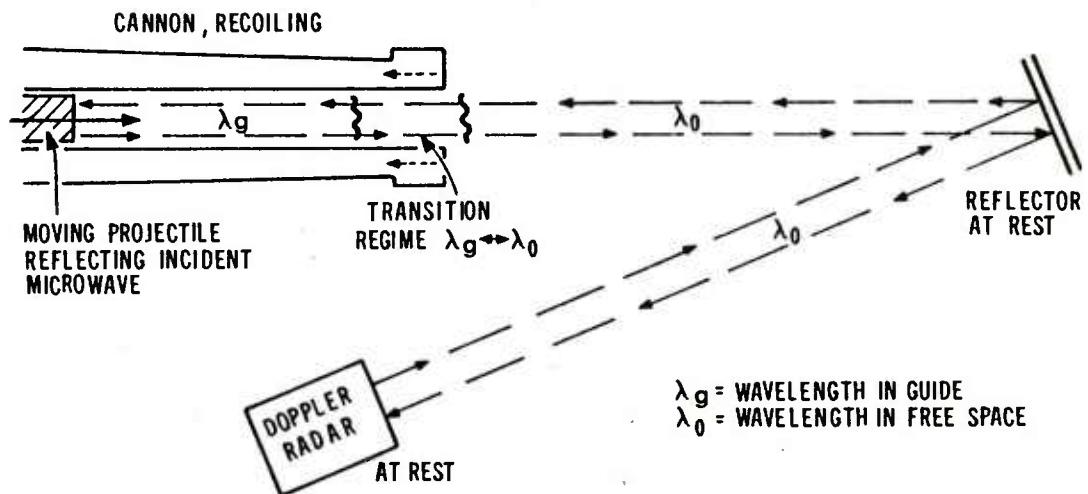
Figure 2.1. Michelson Type Microwave Interferometry Arrangement For The Measurement Of Projectile In-Bore And Launch Motion

the moving boundary and is reflected backward through the waveguide and free space to the receiving antenna. There, the incident wave is brought to interference with the outgoing wave and the resulting phase shift is recorded. The argument of the sinusoidal function varies between zero and 2π, depending on the momentary superposition of the interfering waves. As long as the optical path length of the microwave stays constant, the phase shift also remains constant. When the path length changes, a phase difference occurs. In particular, when the path length of the beam changes by one wavelength, the phase will shift by 2π. Because of the geometrical arrangement, a change in path length by one wavelength corresponds to a displacement of the moving boundary by a half a wavelength, thus allowing us to relate the change in phase to the axial motion of the boundary.

III. SENSITIVITY ANALYSIS, GENERAL

In the experimental arrangement, the waveguide is the gun tube and the moving boundary is the front of the projectile. The wavelength for an infinite circular cylindrical waveguide is given by[2]

[2]D.E. Gray, *American Institute of Physics Handbook,* 3rd ed., McGraw-Hill Book Company, N.Y. 1972.

$$\lambda_g = \lambda_o / [1 - (\lambda_o / \lambda^*)^2]^{\frac{1}{2}}, \text{ with } \lambda_o = c/(nf) \text{ and } \lambda^* = 2\pi a\rho/R, \quad (3.1)$$

where λ_g is the guide wavelength, λ_o is the free space wavelength, λ^* is the cutoff wavelength related to free space, $c = (\mu_o \epsilon_o)^{-\frac{1}{2}}$ is the velocity of light in vacuum, f is the continuous wave frequency, $n = (\mu'\epsilon')^{\frac{1}{2}}$ is the refractive index, $\epsilon'\epsilon_o$ is the permittivity, $\mu'\mu_o$ is the permeability, a is the radius of the waveguide, ρ is a correction factor to account for the helical bore configuration introduced by the rifling, and $R = j_{n,\ell}$ or $j'_{n,\ell}$ is the ℓ-th zero of the Bessel function $J_n(z)$ or its derivative $J'_n(z)$, respectively, depending on the propagating waveguide mode.

These parameters may not stay constant during the interior ballistic propulsion cycle. To analyze the effects of parameter variation on the guide wavelength, we may carry out an error budget analysis. Variation of the parameters in the equation for the guide wavelength yields

$$\Delta\lambda_g / \lambda_g = - [1/(1 - S^2)][\Delta f/f + \Delta n/n]$$

$$- [S^2/(1 - S^2)][\Delta a/a + \Delta\rho/\rho - \Delta R/R],$$

$$S = (\lambda_o / \lambda_g) . \quad (3.2)$$

Since reflection of the microwave on the projectile front may excite higher propagating waveguide modes, R must be considered as a variable. This equation shows that uncertainties in the frequency and the refractive index are increased by $[1/(1 - S^2)]$, whereas uncertainties in the parameters of the cutoff wavelength are amplified by $[S^2/(1 - S^2)]$. The functional behavior of these two amplification factors is shown in Figure 3.1. To illustrate the influence of the microwave frequency selected on the amplification of errors, values for S characteristic to two in-bore microwave interferometry techniques are superimposed. The points marked by TE^*_{11} and TM^*_{01} on the g(s) curves correspond to a technique in which the microwave frequency is chosen such that only one propagation mode can be excited in the gun tube. The lower and upper frequency bounds given are the cutoff frequencies for the TE_{11} and TE_{21} modes and the TM_{01} and TM_{11} modes, respectively. Since we are at the present, mainly concerned with the 105 mm tank gun system, the sensitivity analysis will be arbitrarily restricted to this caliber, thus fixing the waveguide radius. From Figure 3.1 we can see that variations in the frequency or refractivity and in the parameters of the cutoff wavelength are propagated into the guide wavelength with amplifications of $\gtrsim 1.5$ and $\gtrsim 0.6$, respectively, for the single mode technique. The values marked 15 GHz, 105 mm on the g(s) curves refer to the in-bore microwave interferometry arrangement shown

11
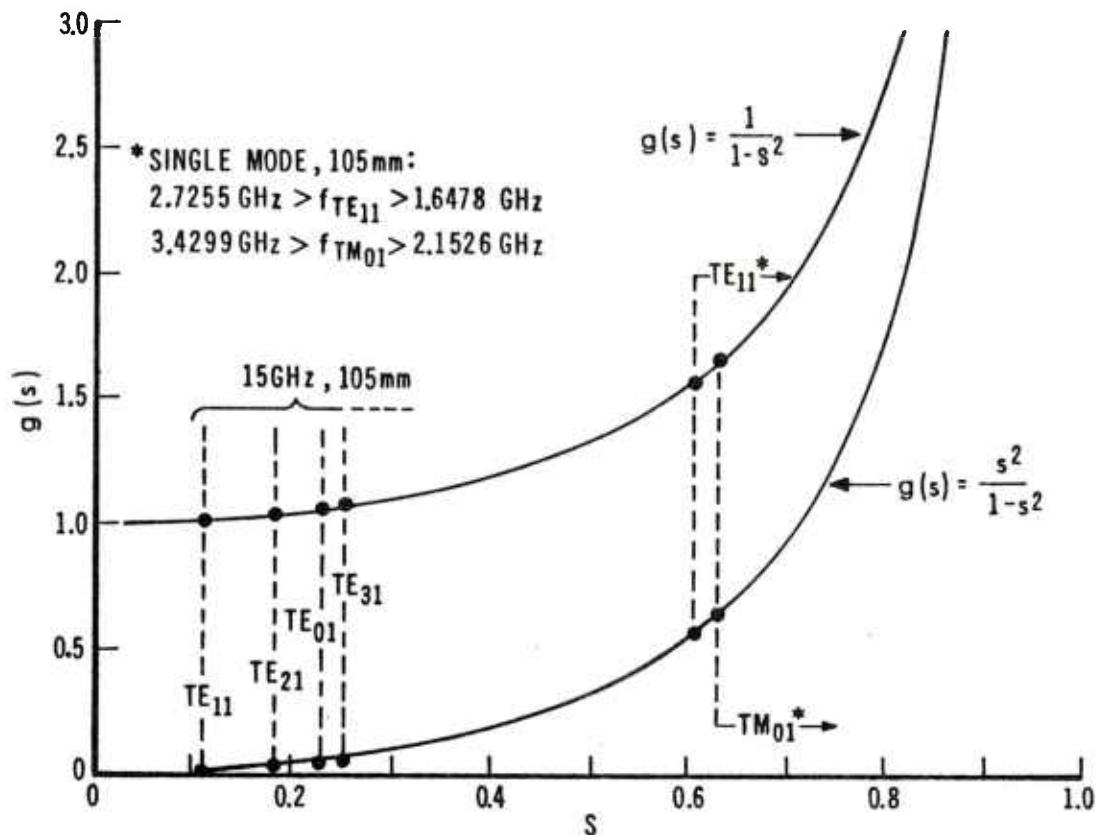
Figure 3.1. Amplification Of Errors In The Guide Wavelength Due
To Variations Of Parameters In The Equation For The
Guide Wavelength

in Figure 2.1, employing a 15 GHz microwave beam which is linearly
polarized in the vertical plane. By going to a higher frequency, the
amplification factor can be reduced substantially. Moreover, an increase
in the carrier frequency well beyond the cutoff frequency of the next
higher propagation mode results in the excitation of a multitude of
propagating modes in the waveguide. Depending on the reflecting surface
most of the available energy will be partitioned into the lowest mode,
thus providing us with an apparent wavelength which fluctuates between
two bounds. Should we be able to design an analysis method which permits
us to extract the contribution from the lowest mode from the microwave
interferometer data, the higher frequency approach would be desireable
for minimizing the error.

To obtain realistic estimates for the variation of the parameters
occurring in the equation for the guide wavelength, two different sets
of data will be used. They will be referred to as shell push data and
M68 firing experiment data.

12

During 1973 a few microwave interferometry measurements were carried out at the Interior Ballistics Division of the Ballistic Research Laboratory by J. W. Evans, where projectiles with different nose configurations were pushed through a shortened 105 mm rifled M68 cannon with a shell pusher machine. Three microwave frequencies, 10 GHz, 35 GHz and 70.65 GHz were used. The interference patterns for the carrier frequencies were recorded as functions of projectile displacement on a chart recorder. In the analysis, data from test #3 (11 Sept. 1973) which employed a flat nosed projectile and 10 GHz and 70.65 GHz microwave simultaneously are used.

The second set of data was collected during Fall and Winter of 1977 by a well instrumented projectile-gun firing experiment[3] which addressed the interior ballistic causes of the erratic flight behavior of M392 type of projectiles when fired from a 105 mm M68 tank gun.

IV. VARIATION IN FREQUENCY

It is common practice to use the frequency as it appears on the frequency meter of the microwave generator as the real microwave frequency. However, this may not be true because the frequency indicator may not be exactly calibrated to the frequency of the microwave generator or the frequency may slightly shift during the operation of the instrumentation. With today's technology, we can safely assume that the last digit in the dial setting is correct within ± 0.5, regardless of the frequency selected. For our 15 GHz radar, that translates into an uncertainty in frequency of $\left| \Delta f/f \right| \leq 0.00033$. The resulting error in the wavelength for the TE_{11} mode is about the same, $\left| \Delta \lambda_g/\lambda_g \right| \leq 0.00034$. Hence, the maximum uncertainty in projectile travel due to this uncertainty is on the order of 0.7 mm for every meter in projectile travel. Generally, the error should be smaller.

The uncertainty in the carrier frequency can completely be eliminated by monitoring the microwave frequency with a counter throughout the experiment - a procedure which will also take out human errors in correctly setting or reading the frequency dial.

V. VARIATION IN REFRACTIVITY

The variability of the refractivity, $N = (n - 1) 10^6$, for microwaves in air has been thoroughly investigated. It can be described by[4]

---

[3] R.K. Loder and J.O. Pilcher, "Nondestructive Test Method To Establish the Performance of Projectile-Gun Systems," Proceedings of the 26-th Defense Conference On Nondestructive Testing, 15 to 17 November 1977, Seattle, Washington; Published by the US Army Materials and Mechanics Research Center, Watertown, Massachusetts.

[4] B.R. Beau and E.J. Dutton, Radio Meteorology, National Bureau of Standards Monograph 92, 1 March 1966.

$$N \equiv (n - 1) \, 10^6 = K_1 P_D/T + K_2 P_W/T + K_3 P_W/T^2, \qquad (5.1)$$

where K_1, K_2 and K_3 are constants, T is the temperature in degrees Kelvin, and P_D and P_W are the partial pressures of dry air and water vapor in mbar, respectively. Using the values for the constants as recommended by Smith and Weintraub[5], the above equation can be expressed by

$$N = (77.6 \, P - 5.6 \, P_W + 3.75 * 10^5 \, P_W/T)/T, \qquad (5.2)$$

where P is the total air pressure, $P = P_D + P_W$. As long as one stays away from frequencies near the water vapor resonance ($f = 22.235$ GHz, $\lambda_0 = 13.5$ mm) and the oxygen resonance ($f = 60.000$ GHz, $\lambda_0 = 5$ mm), the dispersion of the refractive index is within the .5% accuracy limit of the above equation. This equation for the variability of the refractivity has been derived for atmospheric pressures and temperatures up to 250°C. Its applicability for estimating the refractive index of the compressed air column in front of the projectile is highly questionable, even in the absence of blowby gases. However, due to the lack of a suitable approximation or data, the above equation will be used for estimating the order of magnitude in the variation of the wavelength due to the variation in the refractivity, utilizing data obtained from the M68 firing experiment.

With the data given in Table 5.1, we can estimate the variability of the refractive index, using equation (5.2), and, consequently, the change in wavelength for the TE_{11} wave mode propagating in the compressed air column (Table 5.2). The uncertainty in projectile travel due to the change of refractivity in the compressed air column is on the order of a few millimeters and can normally be neglected. However, it exceeds the less than one millimeter accuracy criterion for projectile travel, that is required for the analysis of local tube strains. The estimate of the change in refractivity due to the compressed gas in front of the projectile neglected chemical reactions between the molecular species, electron excitation, activation, dissociation, etc. and did not include blowby gas. The actual error, therefore, could be considerably larger than estimated here.

Figure 5.1 depicts wavelength versus position. The uppermost line corresponds to a guide wavelength with the refractive index set equal to one, which is customarily done in interior ballistics. This vacuum approximation introduces an error in the guide wavelength and projectile travel on the order of

---

[5] *E.K. Smith and S. Weintraub, "The Constants In The Equation For Atmospheric Refractive Index In Radio Frequencies", Proc. IRE41, p 1035-1037.*

TABLE 5.1. DATA PERTAINING TO THE ANALYSIS OF VARIATION IN REFRACTIVITY

ATMOSPHERIC DATA:

T_o = 300°K, P_o = 1.058 $*$ 10^5 Pa, P_{wo} = 3.8 $*$ 10^3 Pa (corresponding to 90% relative humidity)

MICROWAVE FREQUENCIES:

f_1 = 15 GHz and f_2 = 2.725 GHz

WAVEGUIDE PARAMETERS:

2a = 105 mm, ρ = 1.015, R = 1.84 (corresponding to the TE_{11} mode)

SHOCK FRONT AND PROJECTILE MOTION DATA, AVERAGED OVER A POPULATION OF FIVE ROUNDS AND COMPUTED FROM PRESSURE DATA FOR A PROOF SLUG:

1) X_s, [m]	2) ΔX_{sp}, [m]	3) $\overline{\zeta}$	4) $\overline{\pi}$	5) $\overline{\tau}$	6) π_s	7) M_s
3.050	.310	7.23	20.8	2.88	19.4	2.88
4.130	.495	6.69	27.8	4.16	25.2	3.45
5.223	.650	6.67	34.8	5.14	30.7	3.91

1) X_s...location of shock front in cannon, corresponding to pressure gauge positions 12, 16 and 20, respectively; distance is measured from breech end of cannon

2) ΔX_{sp}...length of compressed air column in front of projectile

3) $\overline{\zeta}$ = $(X_s - X_{po})/\Delta X_{sp}$ = $\overline{D}/D_o$...mean density of compressed air column, dimensionless; X_{po} = .821 m is the rest position of the projectile nose in gun tube; $\overline{D}$ is the mean density of the compressed air column; and D_o is the density of the ambient air.

4) $\overline{\pi}$ = $\overline{P}/P_o$...mean pressure of compressed air column, dimensionless.

5) $\overline{\tau}$ = $\overline{\pi}/\overline{\zeta}$ = T/T_o...mean temperature of compressed air column, dimensionless; humid air is assumed as an ideal diatronic gas.

6) π_s = P_s/P_o...measured pressure immediately behind the shockfront, dimensionless.

7) M_s...Mach number for shock velocity

TABLE 5.2.   VARIATION OF GUIDE WAVELENGTH AND PROJECTILE TRAVEL DUE TO
THE CHANGE OF THE REFRACTIVITY IN THE COMPRESSED AIR COLUMN

| X_s [m]	$N * 10^6$	$\Delta n/n_o$ [%]	$\Delta\lambda_{g1}/\lambda_{g1}$ [%]	$\Delta\lambda_{g2}/\lambda_{g2}$ [%]	Δx_1 [mm]	Δx_2 [mm]
3.050	2300	.188	-.190	-.296	1.18	1.84
4.130	2015	.159	-.161	-.251	1.60	2.49
5.223	1961	.154	-.156	-.243	2.03	3.15
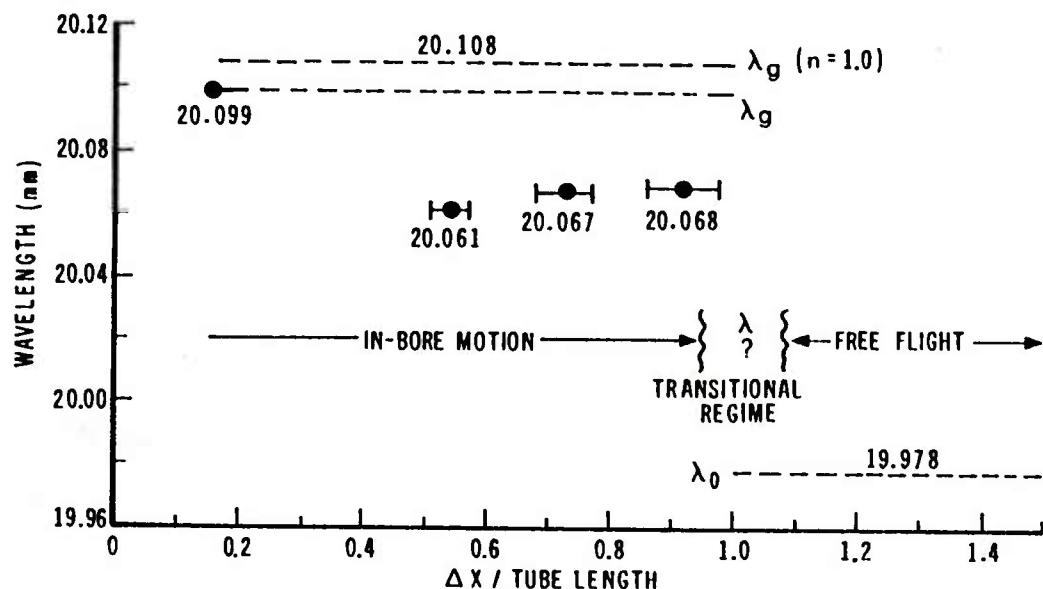
Figure 5.1.   Variation Of Guide Wavelength Due To Variation In Refractivity
For The 105 mm M392 Projectile-M68 Cannon System; Microwave
Parameters: 15 GHz, TE_{11} Propagating Mode

16

$$\Delta\lambda_{g1}/\lambda_{g1} \simeq + 0.043\% , \quad \Delta x_1/x_1 \simeq - 0.085\% , \text{ and}$$

$$\Delta\lambda_{g2}/\lambda_{g2} \simeq + 0.066\% , \quad \Delta x_2/x_2 \simeq - 0.133\% \qquad (5.3)$$

for the two carrier frequencies f_1 and f_2, respectively. The accumulated errors in travel over the total length are about 4 mm and 6.7 mm, respectively. We can eliminate this type of error by monitoring atmospheric pressure, temperature and humidity during the experiment and accounting for them in the data analysis or by measuring the refractivity of the ambient air with a refractometer. The next lower line in Figures 5.1 corresponds to the guide wavelength with the refractive index adjusted to the atmospheric environment. It represents an upper bound for the actual guide wavelength. Estimated mean values for the three selected shock positions are shown underneath. At muzzle exit, the guide wavelength converts back to the free space wavelength. Its functional behavior can be computed from the theory of finite wave guides, in principle. Because of the shock formation and the highly compressed air in front of the projectile, uncertainties in the wavelength will remain for the transitional ballistic regime.

VI. VARIATION IN CUTOFF WAVELENGTH

The variation of the guide wavelength due to the variation of the cutoff wavelength is given by

$$\Delta\lambda_g/\lambda_g = - [S^2/(1 - S^2)][\Delta a/a + \Delta\rho/\rho - \Delta R/R] . \qquad (6.0.1)$$

6.1 Variation of Bore Diameter

The variation of the bore radius is caused by tube wear. Taking the cannon wear profile as obtained in the M68 firing experiment (Figure 6.1), we can approximate the variation in the bore radius as function of projectile nose displacement from the rest position by

$$0.0 \text{ m} \leq \Delta x \leq 1.0 \text{ m}: \quad \Delta a/a \simeq 0.0085 (1 - \Delta x)$$

$$1.0 \text{ m} \leq \Delta x \qquad : \quad \Delta a/a = 0.0 , \qquad (6.1.1)$$

and consequently, estimate the variation in the guide wavelength to be

$$\Delta\lambda_g/\lambda_g = - 0.0085 [S^2/(1 - S^2)](1 - \Delta x). \qquad (6.1.2)$$

17
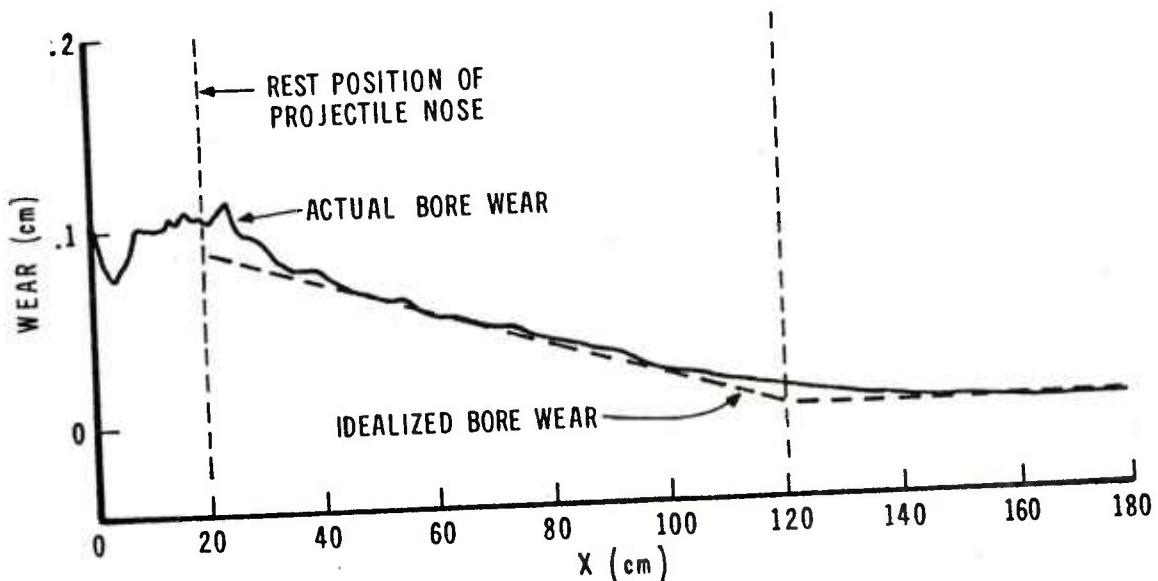
Figure 6.1. Diametral Wear Of The 105 mm M68 Tank Cannon, No. 10328.

The resulting error in projectile travel after one meter of in-bore travel is 0.1 mm and 4.9 mm for the two frequencies f_1 and f_2, respectively. The 105 mm M68 tank cannon example shows that bore wear should be accounted for in large caliber guns, if we employ the single mode technique. The multimode approach, on the other hand, allows us to minimize the error introduced by bore wear by increasing the carrier frequency sufficiently.

6.2 Effect of Bore Rifling

Because most of our gun tubes have a rifled bore, we must expect that the guide wavelength equation derived for a smooth circular cylindrical waveguide is only a first order approximation. A rigorous treatment must account for the helix type of boundary conditions introduced by the rifling. Experiments conducted to determine the effect of para- meter variations on the equation for the guide wavelength suggest that the geometric guide radius has to be replaced by an "electromagnetic radius", thus changing the cutoff frequency by a factor[6]. The correction

---

[6] L. Fortun, "Snelheidsmeting aan projektielen in en direkt buiten een kanon met behulp van Doppler radar," Handleiding Commission van Proefneming deel XA, hoofdstuk 5C-1, s'Gravenhage, July 1963.

18

factor, ρ, must be determined experimentally. Dr. Biele[7] suggested an electromagnetic diameter which is "approximately given by the nominal caliber of the gun plus 1.5 times the groove depth" for the TM_{01} and TE_{11} modes. This formula can be translated into an equation for ρ,

$$\rho = 1 + \kappa \ (\delta a/2a) \ , \tag{6.2.1}$$

where κ is the multiplication factor and δa is the groove depth. This formula yields a value of $\rho = 1.0163$ for the 105 mm tank gun. Experimental electromagnetic diameters obtained by Tengeler[8] for the TE_{11} mode cover this value (Table 6.1).

TABLE 6.1. CORRECTION FACTOR BASED ON TENGELER'S EXPERIMENTAL VALUES FOR ELECTROMAGNETIC DIAMETERS

CANNON		DIAMETER (mm)		ELECTROMAGNETIC DIAMETER (mm), TE_{11} MODE	CORRECTION FACTOR ρ	MULTIPLICATION FACTOR κ	VALUES APPLIED TO 105 mm M68 TANK GUN	
		RIFLING	BORE				MIN. ρ	MAX. ρ
40L60	NEW	41.10	40.03	40.83±.15	1.0200±.0037	1.50±.28	1.0133	1.0194
	WORN		(40.84)	40.89±.15	1.0215±.0037	1.61±.28	1.0145	1.0206
25 pdr	NEW	89.6	87.6	88.75±.15	1.0131±.0017	1.15±.15	1.0109	1.0142
	WORN		(88.4)	89.1±.2	1.0171±.0023	1.50±.20	1.0142	1.0185

To determine a more accurate value for the 105 mm M68 tank gun, an attempt was made to estimate the electromagnetic diameter from the 105 mm shell push data. Unfortunately, the microwave interferometry shell push experiment was only set up for the purpose of measuring the in-bore radar cross section of preselected projectile nose configurations and not for a detailed in-bore microwave propagation study. Since the shell pusher machine had been broken and was not available for conducting the required measurements with all parameters recorded, the data were analyzed to obtain the desired information.

The data were recorded on chart paper; thus, they eluded application of modern data analysis techniques such as numerical filtering, spectral analysis, and general least squares model fitting for determining the guide wavelengths and amplitudes of the individual propagating modes. Because of the large error involved with manually taking values from charts, data averaging was resorted to.

---

[7] J.K. Biele, "Measurement of In-bore Motion of Projectiles And Simultaneous Data Transmission From Built-In Sensors By Means of Microwave Interferometry," Proceedings of the 2nd International Symposium on Ballistics, 9-11 March 1976, Daytona Beach, Florida.

[8] T.I. Tengeler," Het bepalen van de elektrische diameter van kanonnen," Leok-rapporten No. 14.099 en 14.258, Oegstgeest, March/April 1963.

Since the experiment was carried out in an air conditioned room the environment was assumed as 1015 mb pressure (sea level), 25°C temperature and 60% relative humidity, yielding a refractive index of n_o = 1.000366.

The frequencies of the two carrier microwaves as read from the frequency meters of the free running oscillator were assumed to be correct. Taking only those data for which the projectile nose protruded from the muzzle, the following values for the two nominal frequencies were obtained:

$$f_1 = 70.65 \text{ GHz}: \overline{\lambda}_1 = 4.2343 \text{ mm}, \overline{n}_1 = c/(f_1\overline{\lambda}_1) = 1.00214$$

$$\overline{f}_1 = c/(n_o\overline{\lambda}_1) = 70.775 \text{ GHz}$$

$$f_2 = 10.00 \text{ GHz}: \overline{\lambda}_2 = 29.9430 \text{ mm}, \overline{n}_2 = c/(f_2\overline{\lambda}_2) = 1.001211$$

$$\overline{f}_2 = c/(n_o\overline{\lambda}_2) = 10.0084 \text{ GHz} . \tag{6.2.2}$$

Though the frequencies are within the accuracy of the measuring device, the observed discrepancies between the refractivities and between the frequencies suggested that the frequencies or the length scale or both are not quite accurate. Since the measurements were made concurrently, adjustments can be made by minimizing the function

$$F = (f_1 - \hat{f}_1)^2 + (f_2 - \hat{f}_2)^2, \hat{f} - c/(n_o k\overline{\lambda}) . \tag{6.2.3}$$

The length scaling factor k is then determined by

$$k = (c/n_o) [(1/\overline{\lambda}_1)^2 + (1/\overline{\lambda}_2)^2]/[f_1/\overline{\lambda}_1 + f_2/\overline{\lambda}_2] = 1.00175 , \tag{6.2.4}$$

yielding the following values for the free space wavelengths and frequencies for the two carrier microwaves:

$$\lambda_1 = 4.2417 \text{ mm} \qquad \lambda_2 = 29.9954 \text{ mm}$$

$$\hat{f}_1 = 70.6514 \text{ GHz} \qquad \hat{f}_2 = 9.9910 \text{ GHz} . \tag{6.2.5}$$

20

The resulting adjustments in frequency were 0.002% and 0.090%, respectively.

In order to reduce the effect of higher propagating modes on the wavelength for the most dominant mode, the dominant mode was determined as well as the length of the interval required for data averaging. For that purpose, the wavelengths and interference cycles for the first few propagating modes were estimated from the already known information (Tables 6.2 and 6.3), setting $\rho = 1.015$. The interference cycle gives the number of sinusoidal cycles necessary to produce a path change of one wavelength between the two waves.

The interference cycles marked with ● and ■ refer to the TE_{11} and TM_{01} mode, respectively, as the reference mode. The experimental data of the shell push experiment cover approximately 600 and 100 cycles for the two frequencies $\hat{f}_1$ and $\hat{f}_2$ and are given in Figures 6.2 and 6.3, respectively.

TABLE 6.2. INTERFERENCE CYCLES PRODUCED BY PROPAGATING MODES FOR THE CARRIER FREQUENCY

$\hat{f}_1 = 70.6514$ GHz

λ_g, [mm]	MODES		TE_{11}	TM_{01}	TE_{21}	TE_{01} TM_{11}	TE_{31}
4.24287	TE_{11}		✕				
4.24378		TM_{01}	5199	✕			
4.24487	TE_{21}		2116 ●	3568	✕		
4.24672	TE_{01}	TM_{11}	1101 ●	1397 ■	2298	✕	
4.24773	TE_{31}		872 ●	1048	1484	4192	✕
4.25072		TM_{21}	540	603 ■	726	1062	1422

TABLE 6.3. INTERFERENCE CYCLES PRODUCED BY PROPAGATING MODES FOR THE CARRIER FREQUENCY

$\hat{f}_2 = 9.9910$ GHz

| λ_g, [mm]	MODES		TE_{11}	TM_{01}	TE_{21}	TE_{01} TM_{11}	TE_{31}
30.4151	TE_{11}		✕				
30.7225		TM_{01}	98.9	✕			
31.1875	TE_{21}		39.4 ●	66.0	✕		
31.9527	TE_{01}	TM_{11}	19.8 ●	25.0 ■	40.8	✕	
32.3965	TE_{31}		15.4 ●	18.4	25.8	70.0	✕
33.8192		TM_{21}	8.9	9.9 ■	11.2	17.1	22.8
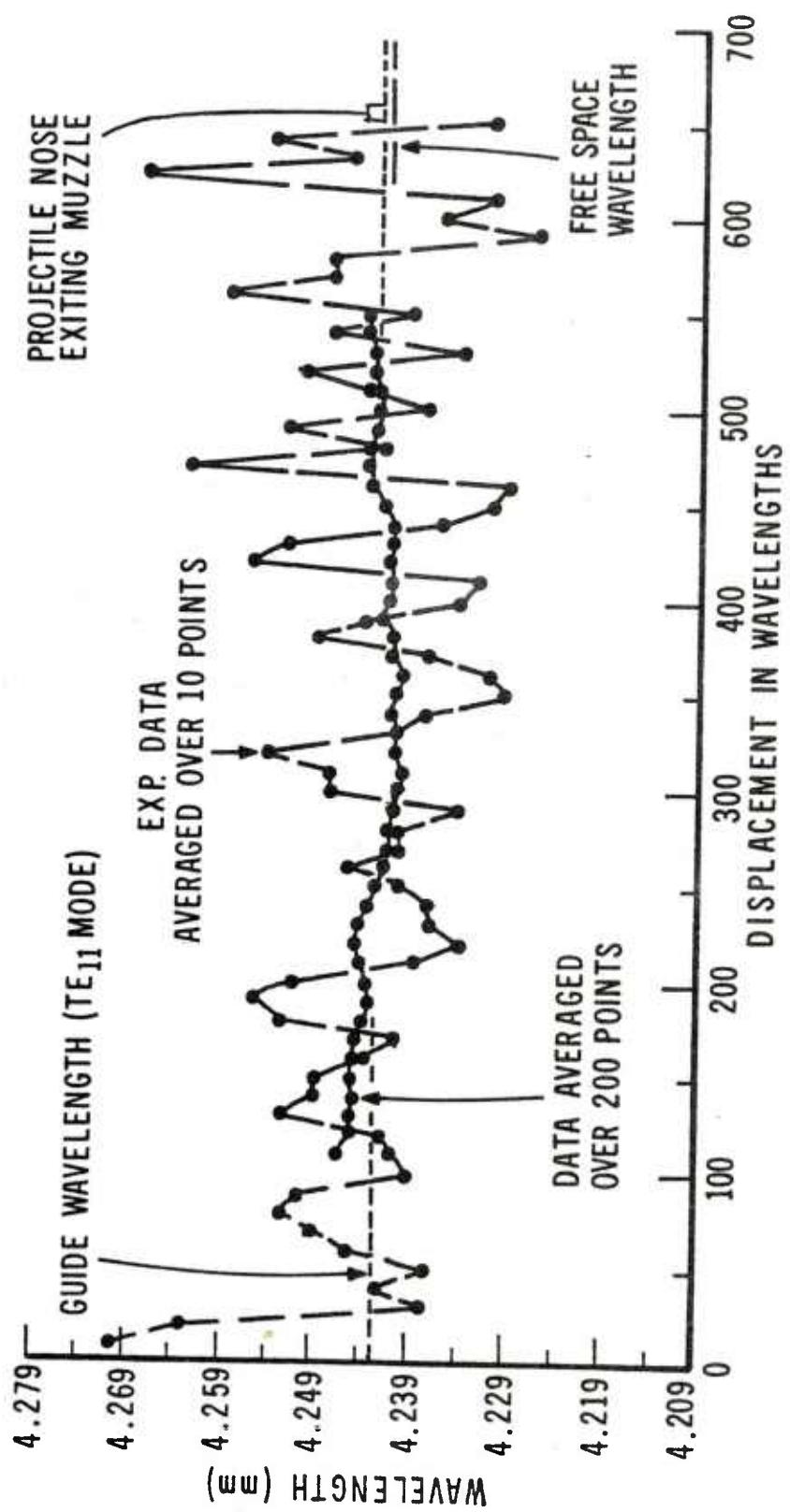
Figure 6.2. Wavelength Versus Projectile In-Bore Displacement For A Microwave Frequency Of 70.6514 GHz.
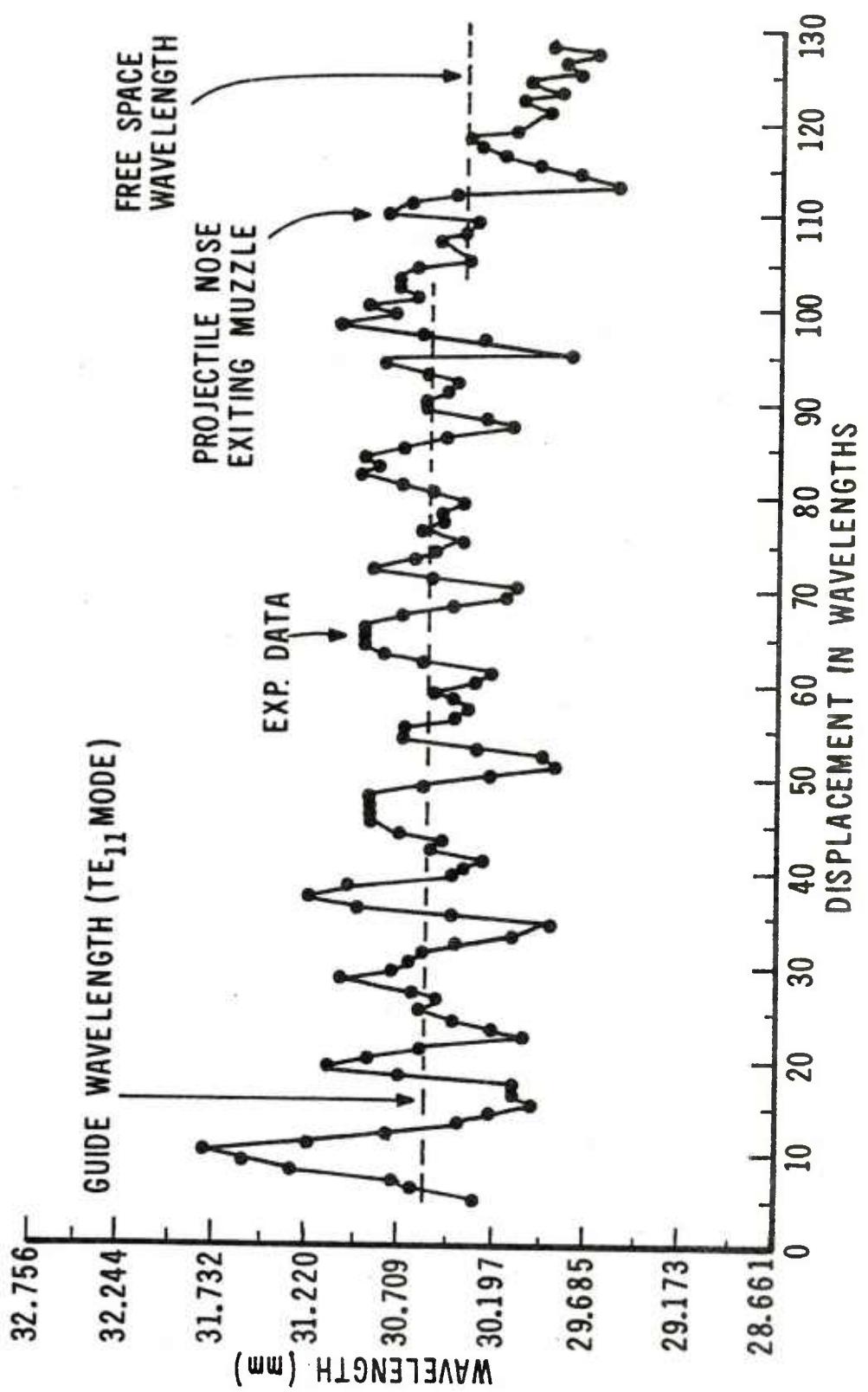
Figure 6.3. Wavelength Versus Projectile In-Bore Displacement For A Microwave Frequency Of 9.9910 GHz

The modulation of wavelength and amplitudes indicates that about one third of the microwave energy is partitioned into the higher propagating modes. To remove this modulation, proper averaging of the data is required. This is not possible for the first data set, because the interference cycles produced by the higher modes exceed by far the number of periods available for averaging. However, for the second data set (f_2 = 9.991 GHz) the situation is reversed. If we select 99 periods as the length for our data, the interval used for averaging will be factors of 2.5, 5.0, and 6.5 larger than the periods for the TE_{21} - TE_{11}, TE_{01} - TE_{11}, and TE_{31} - TE_{11} mode interferences, respectively. Averaging the data over this interval, we obtain for the guide wavelength

$$\bar{\lambda} = 30.41414 \pm 0.00192 \text{ mm} . \tag{6.2.6}$$

The error given corresponds to one standard deviation. Equation 3.1 can be rewritten as

$$\rho = [R/(2\pi a)][c/(n f)]/\{1 - [c/(n f \bar{\lambda})]^2\}^{1/2} , \tag{6.2.7}$$

expressing the correction factor, ρ, as function of parameters which have been determined already. Assuming that ρ is constant over the entire tube length and inserting the appropriate values for the parameters

$$R(TE_{11}) = 1.84118, \quad 2a = 0.105 \text{ m} , \quad c = 2.997925 * 10^8 \text{ m/sec},$$

$$n = 1.000366, \quad f = 9.991 * 10^9 \text{ Hz, and } \bar{\lambda} = 0.03041414 \text{ m} , \tag{6.2.8}$$

we obtain the following estimate for the correction factor

$$\rho = 1.01227 . \tag{6.2.9}$$

This value is in excellent agreement with ρ = 1.01255 ± 0.00165 obtained from Tengeler's data for a new 87.6 mm cannon, but differs by 0.4% from Biele's value which, in turn, agrees with Tengeler's data for a new 40 mm cannon.

Based on the values cited for ρ in the literature and on this analysis, we can safely assume that the uncertainty in the term $\Delta\rho/\rho$ is about 0.004. It will produce a wavelength error on the order of

24

$$\Delta\lambda_{g1}/\lambda_{g1} = \pm\ 0.00005 \text{ for } f_1 = 15 \text{ GHz, and}$$

$$\Delta\lambda_{g2}/\lambda_{g2} = \pm\ 0.00233 \text{ for } f_2 = 2.725 \text{ GHz.} \qquad (6.2.10)$$

The resulting errors in projectile travel are about 0.1 mm and 4.7 mm for one meter of projectile travel, respectively, accumulating to 0.44 mm and 20.5 mm over the total in-bore travel for the 105 mm M68 tank gun. This estimate shows the importance of knowing the exact value of ρ, if we use the single mode approach. With today's instrumentation, recording, and data analysis techniques there is no excuse for not determining the electromagnetic diameter for each gun system in the inventory.

6.3 Effect of Multiple Propagating Modes

The third term in equation (6.0.1), $[S^2/(1 - S^2)](\Delta R/R)$, is identically zero for the single mode method. For the multimode technique, however, we must consider the modulating effect of the higher modes on the lowest propagating wave mode in the waveguide. Since most of the electromagnetic field energy is usually partitioned into the lowest propagating wave mode as indicated by the amplitude variation of the shell push data, the interference with the higher wave modes will cause the apparent wavelength to fluctuate between two bounds. The situation may be aggravated because of the geometry and angular motion of the surface reflecting the microwave. However, the experiment can always be set up such that the energy partition requirement is fulfilled. The error in the displacement measurement will be limited by a constant throughout the length of the tube. The 10 GHz shell push data, for example, exhibit a maximum accumulated error in distance which is for a flat nosed projectile less than 13% of one wavelength at any instant of time. For our sensitivity analysis, we can safely assume that

$$\left|\Delta\lambda_g/\lambda_g\right| = [S^2/(1 - S^2)]\ \left|\Delta R/R\right| \leq 0.15\ \lambda_g \quad , \qquad (6.3.1)$$

limiting the uncertainty in projectile travel due to the multimode approach to 3 mm.

By using a data analysis technique which would permit decomposition of the recorded time series into individual mode components, this oscillating type of error could practically be kept zero. However, no such data analysis approach is yet available.

VII. SUMMARY

Combining all contributions from possible errors as uncertainties in the parameters of the guide wavelength equation, we can establish a bound for the accumulative error in the measurement of projectile travel via microwave interferometry for the 105 mm M68 tank gun example.

TABLE 7.1. UNCERTAINTIES IN THE MEASUREMENT OF PROJECTILE TRAVEL

PARAMETERS IN THE GUIDE WAVELENGTH EQUATION	ESTIMATED UNCERTAINTY IN PROJECTILE TRAVEL, [mm]	
	15 GHz	2.725 GHz
FREQUENCY	3.7	3.7
REFRACTIVE INDEX:		
(a) vacuum approximation	4.0	6.7
(b) compressed air column	2.0	3.2
CUTOFF WAVELENGTH:		
(a) bore wear	.1	4.9
(b) correction for rifling	.5	20.5
(c) multimode technique	3.0	----
ACCUMULATIVE ERROR	13.3	39.0
ACC. ERROR/TOTAL PROJ. IN-BORE TRAVEL	.30%	.89%

These errors are based on uncertainities in our current measurement and data analysis procedures. With relative moderate efforts we can reduce the uncertainty in projectile travel at least by one order of magnitude:

- The carrier frequency of the microwave can be monitored with a frequency counter throughout the experiment. This would practically eliminate any error in the frequency.

- There is no justification in using the vacuum approximation setting the refractive index equal to one. We can determine the index of refraction for air either directly by measuring it with a refractometer or indirectly by calculating it from recorded atmospheric parameters such as pressure, temperature and humidity.

- The error in the refractive index due to the compressed air column with and without blowby gas can, in principle, be determined experimentally. However, a major program would be necessary to accomplish this, especially if we desire quantitative information on obturation.

- The effect of bore wear is relatively small for the 15 GHz case and can be neglected for all practical purposes. For the single mode measurement approach, however, the error introduced by bore wear may not be negligible. The variation of bore diameter as function of tube length can be measured by star gauging, for example, with sufficient accuracy and accounted for in the data analysis.

26

• The uncertainty in the electromagnetic diameter produces an error in the measurement of projectile travel which is relatively small for the 15 GHz multimode case but represents the largest contribution for the 2.725 GHz single mode case. The values cited in the literature for it are too far apart. Hence, the correction factor for the helical structure of the bore should experimentally be determined for each gun system in the inventory as a function of the microwave carrier frequency with an accuracy sufficient to reduce its uncertainty by two orders of magnitude. It is a relatively easy task to design instrumentation which uses an infrared laser interferometer as a displacement reference and readily permits the required measurement. If this measurement is done as an integral part of the firing experiment, the correction factor given as function of axial displacement could even include the effect of bore wear.

• The error introduced by the multimode measurement technique can be eliminated by going to the single mode technique or can be significantly reduced by the use of proper data analysis techniques. Though the multimode measurement technique requires a more complex data analysis procedure than the single mode method, it has the intrinsic advantage that it allows us to reduce the errors in wavelength introduced by parameter uncertainties or variations by sufficiently increasing the microwave carrier frequency.

The sensitivity analysis shows that the currently used measurement procedures lead to uncertainties in projectile in-bore travel which exceed the less than one millimeter accuracy requirement for the analysis of projectile-cannon interface problems. However, the analysis also exhibits that the uncertainty in projectile in-bore travel can be reduced to less than one millimeter, if we employ the microwave measurement technique diligently and ensure proper determination of all parameters in the guide wavelength equation.

27

REFERENCES

1. H. Grumann, "A Microwave Interferometer With Variable Frequency For Continuous Determination of Projectile Motion," Proceedings of Workshop on Projectile-Gun Dynamics under the Auspices of the DEA-G-1060, Ballistics Research and Development, 24-26 April 1979, USA ARRADCOM, Ballistic Research Laboratory, Aberdeen Proving Ground, Maryland 21005 (to be published).

2. D.E. Gray, American Institute of Physics Handbook, 3rd ed., McGraw-Hill Book Company, N.Y. 1972.

3. R.K. Loder and J.O. Pilcher, "Nondestructive Test Method To Establish The Performance Of Projectile-Gun Systems," Proceedings of the 26-th Defense Conference On Nondestructive Testing, 15 to 17 November 1977, Seattle, Washington; Published by the US Army Materials and Mechanics Research Center, Watertown, Massachusetts.

4. B.R. Beau and E.J. Dutton, Radio Meteorology, National Bureau of Standards Monograph, 92, 1 March 1966.

5. E.K. Smith and S. Weintraub, "The Constants In The Equation For Atmospheric Refractive Index In Radio Frequencies," Proc. IRE41, p 1035-1037.

6. L. Fortun, "Snelheidsmeting aan projektielen in en direkt buiten een kanon met behulp van Doppler radar," Handleiding Commission van Proefneming deel XA, hoofdstuk, 5C-1, s'Gravenhage, July 1963.

7. J.K. Biele, "Measurement Of In-Bore Motion Of Projectiles And Simultaneous Data Transmission From Built-In Sensors By Means Of Microwave Interferometry", Proceedings of the 2nd International Symposium on Ballistics, 9-11 March 1976, Daytona Beach, Florida.

8. T.I. Tengeler," Het bepalen van de elektrische diameter van kanonnen," Leok-rapporten No. 14.099 en 14.258, Oegstgeest, March/ April 1963.

DISTRIBUTION LIST

No. of Copies	Organization
12	Commander Defense Technical Info Center ATTN: DDC-DDA Cameron Station Alexandria, VA 22314
2	Director Defense Advanced Research Projects Agency 1400 Wilson Boulevard Arlington, VA 22209
3	Director Defense Nuclear Agency ATTN: STSP (SPLN) STTI STRA (RARP) Washington, DC 20305
1	Commander US Army BMD Advanced Technology Center ATTN: BMDATC-M P. O. Box 1500 Huntsville, AL 35807
1	Commander US Army Materiel Development and Readiness Command ATTN: DRCDMD-ST 5001 Eisenhower Avenue Alexandria, VA 22333
8	Commander US Army ARRADCOM ATTN: DRDAR-LC DRDAR-LCA DRDAR-LCG DRDAR-LCM DRDAR-LCN DRDAR-LCS DRDAR-LCU DRDAR-LCW Dover, NJ 07801

No. of Copies	Organization
5	Commander US Army ARRADCOM ATTN: DRDAR-SC DRDAR-SCA DRDAR-SCF DRDAR-SCM DRDAR-SCS Dover, NJ 07801
17	Commander US Army ARRADCOM ATTN: DRDAR-AC DRDAR-ASP (2 cys) DRDAR-DP (2 cys) DRDAR-FU DRDAR-NS DRDAR-QA (2 cys) DRDAR-SA DRDAR-SE (2 cys) DRDAR-TD DRDAR-TDA DRDAR-TDS DRDAR-TSS (2 cys) Dover, NJ 07801
22	Commander US Army ARRADCOM ATTN: DRDAR-LC, J.T. Frasier DRDAR-LCA, W. Benson S. Bernstein S.H. Chu G. Demitrack B. Knutelski C. Larsen K. Reuben L. Rosendorf S. Westley W. Williver S. Yim DRDAR-LCS, J. Gregorits K. Rubin DRDAR-LCU, E. Barrieres W. Bunting R. Carr R. Davitt F. Diorio E.H. Moore J. Sikra M. Weinstock

DISTRIBUTION LIST

No. of Copies	Organization

22	Commander
	US Army ARRADCOM
	ATTN: DRDAR-SC, D. Gyorog
	     DRDAR-SCA, M. Chu
	       W. Gadomski
	       S. Goldstein
	       E. Jeeter
	       H. Kahn
	       S. Langdo
	       E. Malatesta
	       C.J. McGee
	       F.P. Puzycki
	       R. Rhoades
	       R. Schlenner
	     DRDAR-SCF, L. Berman
	       B. Brodman
	       G. Del Coco
	       K. Pfleger
	       M.J. Schmitz
	        DRDAR-SCM, E. Bloore
	          J. Mulherin
	        DRDAR-SCS, J. Blumer
	          D. Brandt
	          T. Hung
	          S. Jacobson
	Dover, NJ 07801

9	Commander
	US Army ARRADCOM
	Benet Weapons Laboratory
	ATTN: DRDAR-LCB, T. Allen
	       R. Billington
	       T. Davidson
	       P. O'Hara
	       T. Simkins
	       P. Vottis
	       J. Wu
	       J. Zweig
	     DRDAR-LCB-T
	Watervliet, NY 12189

1	Commander US Army Armament Materiel Readiness Command ATTN: DRDAR-LEP-L, Tech Lib Rock Island, IL 61299

No. of Copies	Organization
1	Commander US Army Aviation Research and Development Command ATTN: DRDAV-E 4300 Goodfellow Blvd. St. Louis, MO 63120
1	Director US Army Air Mobility Research and Development Laboratory Moffett Field, CA 94035

2	Director
	US Army Research and
	  Technology Laboratories
	  (AVRADCOM)
	Ames Research Center
	Moffett Field, CA 94035

1	Commander US Army Communications Research and Development Command ATTN: DRDCO-PPA-SA Fort Monmouth, NJ 07703
1	Commander US Army Electronics Research and Development Command Technical Support Activity ATTN: DELSD-L Fort Monmouth, NJ 07703
1	Commander US Army Harry Diamond Laboratories 2800 Powder Mill Road Adelphi, MD 20783

3	Commander
	US Army Harry Diamond Laboratories
	ATTN: DELHD-I-TR, H.D. Curchak,
	                H. Davis
	     DELHD-S-DE-ES, Ben Banner
	2800 Powder Mill Road
	Adelphi, MD 20783

DISTRIBUTION LIST

No. of Copies	Organization	No. of Copies	Organization

3	Commander
	US Army Missile Command
	ATTN: DRSMI-R
	       DRSMI-RBL
	       DRSMI-YDL
	Redstone Arsenal, AL 35809
		2	Project Manager
			XM-1 Tank Dequindre
			Detroit, MI 48207

2	Commander US Army Mobility Equipment Research and Development Command Fort Belvoir, VA 22060	2	Project Manager Nuclear Munitions ATTN: DRCPM-NUC Dover, NJ 07801

2	Commander
	US Army Tank Automotive Research
	   and Development Command
	ATTN: DRDTA-UL
	       Technical Director
	Warren, MI 48090
		2	Project Manager
			Tank Main Armament Systems
			ATTN: DRCPM-TMA
			Dover, NJ 07801

2	Commander US Army Jefferson Proving Ground ATTN: STEJP-TD-O STEJP-TD-E Madison, IN 47250	2	Project Manager Division Air Defense Gun ATTN: DRCPM-ADG Dover, NJ 07801
2	Director US Army TRADOC Systems Analysis Activity ATTN: ATAA-SL, Tech Lib White Sands Missile Range, NM 88002	3	Project Manager Cannon Artillery Weapons Systems ATTN: DRCPM-CAWS Dover, NJ 07801
2	Commander US Army Yuma Proving Ground ATTN: STEYP-MTW YUMA, AZ 85364	1	Product Manager for 30mm Ammo. ATTN: DRCPM-AAH-30mm Dover, NJ 07801
2	Commander US Army Research Office P.O. Box 12211 ATTN: D.G. Manges F.W. Schmiedeshoff Research Triangle Park, NC 27709	2	Product Manager M110E2 Weapon System, DARCOM ATTN: DRCPM-M110E2 Rock Island, IL 61299

1	Program Manager
	Advanced Attack Helicopter, DARCOM
	4300 Good Fellow Boulevard
	St. Louis, MO 63166
		4	Director
			US Army Mechanics and
			   Materials Research Center
			ATTN: Director (3 cys)
			       DRXMR-ATL (1 cy)
			Watertown, MA 02172

		1	Commander Naval Air Systems Command ATTN: AIR-604 Washington, DC 20360
		1	Commander Naval Sea Systems Command Washington, DC 20362

No. of Copies	Organization	No. of Copies	Organization
2	Commander Naval Sea Systems Command (NAVSEA-9941) ATTN: L. Pasiuk Washington, DC 20362	5	Commander Naval Surface Weapons Center ATTN: Code G-33, T.N. Tschirn Code N-43, J.J. Yagla L. Anderson G. Soo Hoo Code TX, Dr. W.G. Soper Dahlgren, VA 22448
1	Superintendent Naval Postgraduate School ATTN: Dir of Lib Monterey, CA 93940	2	Commander Naval Weapons Center China Lake, CA 93555
1	Commander Naval Air Development Center Johnsville Warminster, PA 18974	3	Commander Naval Weapons Center ATTN: J. O'Malley D. Potts R.G. Sewell China Lake, CA 93555
1	Commander Naval Missile Center Point Mugu, CA 95041	1	Commander Naval Ordnance Station Indian Head, MD 20640
1	Commander Naval Research Laboratory ATTN: Code 7908, A.E. Williams Washington, DC 20375	2	Commander Naval Ordnance Station ATTN: Code 5034, Ch Irish, Jr. T.C. Smith Indian Head, MD 20640
2	Commander David W. Taylor Naval Ship Research and Development Ctr Bethesda, MD 20084	2	Commander Marine Corps Development and Education Command (MCDEC) ATTN: MCDEC/D-092 MCDEC/LAV Directorate Quantico, VA 22134
2	Commander Naval Surface Weapons Center ATTN: G-13, W.D. Ralph Dahlgren, VA 22448	4	Commander US Air Force Armament Laboratory ATTN: AFATL-DLA, W. Dittrich AFATL-DLD, D. Davis AFATL-DLDL, O. Heiney G. Winchenbach Eglin AFB, FL 32542
3	Commander Naval Surface Weapons Center ATTN: Code E-31, R.C. Reed M.T. Walchak Code V-14, W.M. Hinckley Silver Spring, MD 20910	2	Commander US Air Force Weapons Laboratory ATTN: AFWL-SUL Kirtland AFB, NM 87117
2	Commander Naval Surface Weapons Center Silver Spring, MD 20910		

DISTRIBUTION LIST

No. of Copies	Organization
2	Director Lawrence Livermore Laboratory ATTN: LIB. L-368, C. Honodel P.O. Box 808 Livermore, CA 94550
1	Director Los Alamos Scientific Laboratory Los Alamos, NM 85744
2	Director Sandia Laboratories ATTN: LIB. Div 5534, L.C. Chhabildas Albuquerque, NM 87185
1	Headquarters National Aeronautics and Space Administration Washington, DC 20546
1	Director National Aeronautics and Space Administration Ames Research Center ATTN: N237-1, C. DeRose Moffett Field, CA 94035
1	Director National Aeronautics and Space Administration Lyndon B. Johnson Space Center ATTN: Library Houston, TX 77058
2	Director National Aeronautics and Space Administration Langley Research Center Langley Station Hampton, VA 23365

No. of Copies   Organization

Aberdeen Proving Ground

Dir, USAMSAA
  ATTN: DRXSY-D
          DRXSY-MP, H. Cohen
          DRXSY-G, E. Christman
          DRXSY-OSD, H. Burke
          DRXSY-G, R.C. Conroy
          DRXSY-LM, J.C.C. Fine
Cdr, USATECOM
  ATTN: DRSTE-TO-F
Dir, USACSL, Bldg. E3516, EA
  ATTN: DRDAR-CLB-PA
          DRDAR-CL
          DRDAR-CLD
          DRDAR-CLB
          DRDAR-CLY
          DRDAR-CLN
Dir, USAHEL
  ATTN: A.H. Eckles, III
Dir, Materiel Testing Directorate
  ATTN: STEAP-MT-G

USER EVALUATION OF REPORT

Please take a few minutes to answer the questions below; tear out this sheet, fold as indicated, staple or tape closed, and place in the mail. Your comments will provide us with information for improving future reports.

1. BRL Report Number _____

2. Does this report satisfy a need? (Comment on purpose, related project, or other area of interest for which report will be used.)

_____

_____

_____

3. How, specifically, is the report being used? (Information source, design data or procedure, management procedure, source of ideas, etc.)_____

_____

_____

4. Has the information in this report led to any quantitative savings as far as man-hours/contract dollars saved, operating costs avoided, efficiencies achieved, etc.? If so, please elaborate.

_____

_____

5. General Comments (Indicate what you think should be changed to make this report and future reports of this type more responsive to your needs, more usable, improve readability, etc.)_____

_____

_____

_____

6. If you would like to be contacted by the personnel who prepared this report to raise specific questions or discuss the topic, please fill in the following information.

Name: _____

Telephone Number: _____

Organization Address: _____

_____

_____